Cosmological Implications of Scalar Tensor Theories

Lavrentios Kazantzidis

PhD Defence

Section of Theoretical Physics, Department of Physics, University of Ioannina

22 March 2022

Ioannina

Publication Record

Evolution of the $f\sigma_8$ tension with the Planck15/ΛCDM determination and implications for modified gravity theories

Lavrentios Kazantzidis, Leandros Perivolaropoulos (Mar 4, 2018)

Published in: *Phys.Rev.D* 97 (2018) 10, 103503 • e-Print: 1803.01337 [astro-ph.CO]

Consistency of modified gravity with a decreasing $G_{\rm eff}(z)$ in a ΛCDM background

Radouane Gannouji (Valparaiso U., Catolica), Lavrentios Kazantzidis (Ioannina U.), Leandros Perivolaropoulos (Ioannina U.), David Polarski (U. Montpellier, L2C) (Sep 19, 2018)

Published in: *Phys.Rev.D* 98 (2018) 10, 104044 • e-Print: 1809.07034 [gr-qc]

Constraining power of cosmological observables: blind redshift spots and optimal ranges

L. Kazantzidis (Ioannina U.), L. Perivolaropoulos (Ioannina U.), F. Skara (Ioannina U.) (Dec 13, 2018)

Published in: *Phys.Rev.D* 99 (2019) 6, 063537 • e-Print: 1812.05356 [astro-ph.CO]

Hints of modified gravity in cosmos and in the lab?

Leandros Perivolaropoulos (Ioannina U.), Lavrentios Kazantzidis (Ioannina U.) (Jan 25, 2019)

Published in: *Int.J.Mod.Phys.D* 28 (2019) 05, 1942001 • e-Print: 1904.09462 [gr-qc]

σ_8 Tension. Is Gravity Getting Weaker at Low z? Observational Evidence and Theoretical Implications

Lavrentios Kazantzidis (Ioannina U.), Leandros Perivolaropoulos (Ioannina U.) (Jul 6, 2019)

e-Print: 1907.03176 [astro-ph.CO]

Publication Record

Evolution of the $f\sigma_8$ tension with the Planck15/ΛCDM determination and implications for modified gravity theories
Lavrentios Kazantzidis, Leandros Perivolaropoulos (Mar 4, 2018)
Published in: *Phys.Rev.D* 97 (2018) 10, 103503 • e-Print: 1803.01337 [astro-ph.CO]

Consistency of modified gravity with a decreasing $G_{\rm eff}(z)$ in a ΛCDM background
Radouane Gannouji (Valparaiso U., Catolica), Lavrentios Kazantzidis (Ioannina U.), Leandros Perivolaropoulos (Ioannina U.), David Polarski (U. Montpellier, L2C) (Sep 19, 2018)
Published in: *Phys.Rev.D* 98 (2018) 10, 104044 • e-Print: 1809.07034 [gr-qc]

Constraining power of cosmological observables: blind redshift spots and optimal ranges
L. Kazantzidis (Ioannina U.), L. Perivolaropoulos (Ioannina U.), F. Skara (Ioannina U.) (Dec 13, 2018)
Published in: *Phys.Rev.D* 99 (2019) 6, 063537 • e-Print: 1812.05356 [astro-ph.CO]

Hints of modified gravity in cosmos and in the lab?
Leandros Perivolaropoulos (Ioannina U.), Lavrentios Kazantzidis (Ioannina U.) (Jan 25, 2019)
Published in: *Int.J.Mod.Phys.D* 28 (2019) 05, 1942001 • e-Print: 1904.09462 [gr-qc]

σ_8 Tension. Is Gravity Getting Weaker at Low z? Observational Evidence and Theoretical Implications
Lavrentios Kazantzidis (Ioannina U.), Leandros Perivolaropoulos (Ioannina U.) (Jul 6, 2019)
e-Print: 1907.03176 [astro-ph.CO]

Hints of a Local Matter Underdensity or Modified Gravity in the Low z Pantheon data
L. Kazantzidis (Ioannina U.), L. Perivolaropoulos (Ioannina U.) (Apr 5, 2020)
Published in: *Phys.Rev.D* 102 (2020) 2, 023520 • e-Print: 2004.02155 [astro-ph.CO]

H_0 tension, phantom dark energy, and cosmological parameter degeneracies
G. Alestas (Ioannina U.), L. Kazantzidis (Ioannina U.), L. Perivolaropoulos (Ioannina U.) (Apr 23, 2020)
Published in: *Phys.Rev.D* 101 (2020) 12, 123516 • e-Print: 2004.08363 [astro-ph.CO]

Hints for possible low redshift oscillation around the best-fitting ΛCDM model in the expansion history of the Universe
L. Kazantzidis, H. Koo, S. Nesseris, L. Perivolaropoulos, A. Shafieloo (Oct 7, 2020)
Published in: *Mon.Not.Roy.Astron.Soc.* 501 (2021) 3, 3421-3426 • e-Print: 2010.03491 [astro-ph.CO]

$w-M$ phantom transition at z_t <0.1 as a resolution of the Hubble tension
George Alestas (Ioannina U.), Lavrentios Kazantzidis (Ioannina U.), Leandros Perivolaropoulos (Ioannina U.) (Dec 27, 2020)
Published in: *Phys.Rev.D* 103 (2021) 8, 083517 • e-Print: 2012.13932 [astro-ph.CO]

Late-transition vs smooth $H(z)$ deformation models for the resolution of the Hubble crisis
George Alestas (Ioannina U.), David Camarena, Eleonora Di Valentino (Sheffield U.), Lavrentios Kazantzidis (Ioannina U.), Valerio Marra (Trieste Observ. and IFPU, Trieste) et al. (Oct 8, 2021)
e-Print: 2110.04336 [astro-ph.CO]

Observational constraints on the deceleration parameter in a tilted universe
Kerkyra Asvesta, Lavrentios Kazantzidis, Leandros Perivolaropoulos, Christos G. Tsagas (Feb 2, 2022)
e-Print: 2202.00962 [astro-ph.CO]

# of Citations: 479, h-index: 11

Publications Presented in the Talk

- L. Kazantzidis and L. Perivolaropoulos, **Phys.Rev.D** 97 (2018) 10, 103503.
- R. Gannouji, L. Kazantzidis, L. Perivolaropoulos and D. Polarski, **Phys.Rev.D** 98 (2018) 10, 104044.
- L. Kazantzidis and L. Perivolaropoulos, **Phys.Rev.D** 102 (2020) 2, 023520.
- L. Kazantzidis, H. Koo, S. Nesseris, L. Perivolaropoulos and A. Shafieloo, **Mon.Not.Roy.Astron.Soc.** 501 (2021) 3, 34216.
- G. Alestas, D. Camarena, E. Di Valentino, L. Kazantzidis, V. Marra, S. Nesseris and L. Perivolaropoulos, to appear in **Phys.Rev.D**.

https://cosmology.physics.uoi.gr

Overview

The Standard Cosmological Model - ΛCDM

- The basic assumptions of this model are
  - The validity of General Relativity (GR).

The Standard Cosmological Model - ΛCDM

- The basic assumptions of this model are
  - The validity of General Relativity (GR).
  - Homogeneity and Isotropy.

The Standard Cosmological Model - ΛCDM

- The basic assumptions of this model are
  - The validity of General Relativity (GR).
  - Homogeneity and Isotropy.
  - Flatness of spacetime.

The Standard Cosmological Model - ΛCDM

- The basic assumptions of this model are
  - The validity of General Relativity (GR).
  - Homogeneity and Isotropy.
  - Flatness of spacetime.
  - A primitive phase of cosmic inflation (a period of rapid accelerated expansion) in order to address the horizon and flatness problems.

The Standard Cosmological Model - ΛCDM

- The basic assumptions of this model are
  - The validity of General Relativity (GR).
  - Homogeneity and Isotropy.
  - Flatness of spacetime.
  - A primitive phase of cosmic inflation (a period of rapid accelerated expansion) in order to address the horizon and flatness problems.
  - The existence of Cold Dark Matter (CDM).

The Standard Cosmological Model - ΛCDM

- The basic assumptions of this model are
  - The validity of General Relativity (GR).
  - Homogeneity and Isotropy.
  - Flatness of spacetime.
  - A primitive phase of cosmic inflation (a period of rapid accelerated expansion) in order to address the horizon and flatness problems.
  - The existence of Cold Dark Matter (CDM).
  - The existence of the cosmological constant (Λ). The cosmological constant drives the observed accelerated expansion of the Universe.

The Standard Cosmological Model - ΛCDM

- The basic assumptions of this model are
  - The validity of General Relativity (GR).
  - Homogeneity and Isotropy.
  - Flatness of spacetime.
  - A primitive phase of cosmic inflation (a period of rapid accelerated expansion) in order to address the horizon and flatness problems.
  - The existence of Cold Dark Matter (CDM).
  - The existence of the cosmological constant (Λ). The cosmological constant drives the observed accelerated expansion of the Universe.
- ΛCDM remains until now the simplest model that is consistent with a wide range of experiments/observations from millimetre scales up to galactic scales and beyond.

The Standard Cosmological Model - ΛCDM

- The basic assumptions of this model are
  - The validity of General Relativity (GR).
  - Homogeneity and Isotropy.
  - Flatness of spacetime.
  - A primitive phase of cosmic inflation (a period of rapid accelerated expansion) in order to address the horizon and flatness problems.
  - The existence of Cold Dark Matter (CDM).
  - The existence of the cosmological constant (Λ). The cosmological constant drives the observed accelerated expansion of the Universe.
- ΛCDM remains until now the simplest model that is consistent with a wide range of experiments/observations from millimetre scales up to galactic scales and beyond.
- However, despite its simplicity, consistency with the cosmological data and accurately predicting a variety of different phenomena, ΛCDM faces a number of challenges both at the theoretical and the observational level.

Theoretical Challenges of ΛCDM

From the point of view of particle physics, the cosmological constant naturally emerges as an energy density of the vacuum, since both the cosmological constant and the vacuum energy present the same dynamical behaviour in the context of GR. The most important theoretical difficulties correspond to:

Theoretical Challenges of ΛCDM

From the point of view of particle physics, the cosmological constant naturally emerges as an energy density of the vacuum, since both the cosmological constant and the vacuum energy present the same dynamical behaviour in the context of GR. The most important theoretical difficulties correspond to:

- The Cosmological Constant (or Smallness) Problem: This problem refers to the inconsistency of the observed energy density of the cosmological constant $\rho_\Lambda \approx 10^{-47}\ GeV^4$ with the energy density of the vacuum $\rho_{vac} \approx 10^{74}\ GeV^4$ which is 10^{121} orders of magnitude.

Theoretical Challenges of ΛCDM

From the point of view of particle physics, the cosmological constant naturally emerges as an energy density of the vacuum, since both the cosmological constant and the vacuum energy present the same dynamical behaviour in the context of GR. The most important theoretical difficulties correspond to:

- The Cosmological Constant (or Smallness) Problem: This problem refers to the inconsistency of the observed energy density of the cosmological constant $\rho_\Lambda \approx 10^{-47}\ GeV^4$ with the energy density of the vacuum $\rho_{vac} \approx 10^{74}\ GeV^4$ which is 10^{121} orders of magnitude.
- The Cosmic Coincidence Problem: The cosmic coincidence problem can be summarized in the following question: Why the present values of the energy densities of the cosmological constant and of matter are of the same order of magnitude, *i.e.* $\rho_{\Lambda,0}/\rho_{m,0} \sim \mathcal{O}(1)$.

Observational Challenges of ΛCDM (1/2)

- The best fit parameter values of ΛCDM have been reported by a plethora of missions. Perhaps the most known corresponds to the Planck mission which uses CMB+BAO data to constrain the six basic parameters of ΛCDM to an extreme accuracy. As a result in the context of GR the current concordance model is known as Planck/ΛCDM.

Parameter	Name	Value
$\Omega_{\mathrm{b},0}\, h^2$	Baryon Density	0.02237 ± 0.00015
$\Omega_{\mathrm{c},0}\, h^2$	Cold Dark Matter Density	0.1200 ± 0.0012
$100\,\theta_{MC}$	Angular Size of the Sound Horizon at Recombination	1.04092 ± 0.00031
τ	Optical Depth	0.0544 ± 0.0073
$ln(10^{10}\, A_s)$	Amplitude of Curvature Primordial Perturbations	3.044 ± 0.014
n_s	Spectral Index	0.9649 ± 0.0042

Observational Challenges of ΛCDM (1/2)

- The best fit parameter values of ΛCDM have been reported by a plethora of missions. Perhaps the most known corresponds to the Planck mission which uses CMB+BAO data to constrain the six basic parameters of ΛCDM to an extreme accuracy. As a result in the context of GR the current concordance model is known as Planck/ΛCDM.

Parameter	Name	Value
$\Omega_{\mathrm{b},0}\, h^2$	Baryon Density	0.02237 ± 0.00015
$\Omega_{\mathrm{c},0}\, h^2$	Cold Dark Matter Density	0.1200 ± 0.0012
$100\,\theta_{MC}$	Angular Size of the Sound Horizon at Recombination	1.04092 ± 0.00031
τ	Optical Depth	0.0544 ± 0.0073
$ln(10^{10}\, A_s)$	Amplitude of Curvature Primordial Perturbations	3.044 ± 0.014
n_s	Spectral Index	0.9649 ± 0.0042

- Observationally, a number of different cosmological datasets analysed in the last decade seem to prefer different values (at a level of 2σ or more) for some of the basic parameters of Planck/ΛCDM.

Planck Collaboration, Astron.Astrophys. 641 (2020) A6,

Observational Challenges of ΛCDM (2/2)

The most important "tensions" of Planck/ΛCDM include the following:

- The H_0 Tension: The first tension refers to the mismatch of the value of the Hubble constant

H_0 **Tension**	Planck Measurement	Supernova Measurement
H_0	$67.36 \pm 0.54\ km\ s^{-1}\ Mpc^{-1}$	$73.04 \pm 1.04\ km\, s^{-1}\ Mpc^{-1}$

The tension is at a 5σ level

Observational Challenges of ΛCDM (2/2)

The most important "tensions" of Planck/ΛCDM include the following:

- The H_0 Tension: The first tension refers to the mismatch of the value of the Hubble constant

H_0 **Tension**	Planck Measurement	Supernova Measurement
H_0	$67.36 \pm 0.54\ km\, s^{-1}\ Mpc^{-1}$	$73.04 \pm 1.04\ km\, s^{-1}\ Mpc^{-1}$

The tension is at a 5σ level

- The S_8 or Growth Tension: This is a milder tension and refers to mismatch of the values of the parameter $S_8 \equiv \sigma_8 \sqrt{\Omega_{\mathrm{m},0}/0.3}$, where σ_8 corresponds to the density rms fluctuations within spheres of radius $R = 8h^{-1} Mpc$.

S_8 **Tension**	Planck Measurement	Weak Lensing Measurement
$S_8 = \sigma_8 \sqrt{\Omega_{\mathrm{m},0}/0.3}$	0.834 ± 0.016	$0.766^{+0.020}_{-0.014}$, $0.79^{+0.05}_{-0.04}$

The tension is at a $2-3\sigma$ level

Planck Collaboration, Astron.Astrophys. 641 (2020) A6, A. Riess et al, arXiv:2112.04510,
DES Collaboration Mon.Not.Roy.Astron.Soc. 488 (2019), 4779, KiDS Collaboration Astron.Astrophys. 646, A140 (2021)

Observational Challenges of ΛCDM (2/2)

The most important "tensions" of Planck/ΛCDM include the following:

- The H_0 Tension: The first tension refers to the mismatch of the value of the Hubble constant

H_0 **Tension**	Planck Measurement	Supernova Measurement
H_0	67.36 ± 0.54 $km\, s^{-1}\ Mpc^{-1}$	73.04 ± 1.04 $km\, s^{-1}\ Mpc^{-1}$

  The tension is at a 5σ level

- The S_8 or Growth Tension: This is a milder tension and refers to mismatch of the values of the parameter $S_8 \equiv \sigma_8 \sqrt{\Omega_{\mathrm{m},0}/0.3}$.

S_8 **Tension**	Planck Measurement	Weak Lensing Measurement
$S_8 = \sigma_8\sqrt{\Omega_{\mathrm{m},0}/0.3}$	0.834 ± 0.016	$0.766^{+0.020}_{-0.014}$, $0.79^{+0.05}_{-0.04}$

  The tension is at a $2-3\sigma$ level

As a result, a vast variety of ideas have been proposed in the literature in order to address the aforementioned (theoretical or observational) tensions. A simple way to account for the existing tensions is to allow for the possibility of extensions of GR in the form of modified theories of gravity.

Growth Data: Observational Probe of Perturbations (1/2)

The RSD data probe the growth of perturbations. Actually the data are obtained by detecting the distortions of the power spectrum of perturbations which are induced by peculiar velocities

Growth Data: Observational Probe of Perturbations (1/2)

The RSD data probe the growth of perturbations. Actually the data are obtained by detecting the distortions of the power spectrum of perturbations which are induced by peculiar velocities

The growth rate of perturbations $f(a)$ is defined as

$$f(a) = \frac{dln\delta(a)}{dlna} \text{ where } \delta(a) \equiv \frac{\delta\rho_m}{\rho_m} \text{ is the linear matter overdensity growth factor} \tag{1}$$

and ρ_m is the background matter density.

Combining Eq.(1) with the density rms fluctuations within spheres of radius $R = 8h^{-1}Mpc$, i.e.

$$\sigma(a) = \sigma_8 \frac{\delta(a)}{\delta(1)} \tag{2}$$

Growth Data: Observational Probe of Perturbations (1/2)

The RSD data probe the growth of perturbations. Actually the data are obtained by detecting the distortions of the power spectrum of perturbations which are induced by peculiar velocities

The growth rate of perturbations $f(a)$ is defined as

$$f(a) = \frac{dln\delta(a)}{dlna} \text{ where } \delta(a) \equiv \frac{\delta\rho_m}{\rho_m} \text{ is the linear matter overdensity growth factor} \tag{1}$$

and ρ_m is the background matter density.

Combining Eq.(1) with the density rms fluctuations within spheres of radius $R = 8h^{-1}Mpc$, i.e.

$$\sigma(a) = \sigma_8 \frac{\delta(a)}{\delta(1)} \tag{2}$$

The observable product $f\sigma_8(a)$ that is published by various surveys corresponds to

$$f\sigma_8(a) \equiv f(a) \cdot \sigma(a) = \frac{\sigma_8}{\delta(1)}\ a\ \delta'(a) \tag{3}$$

Growth Data: Observational Probe of Perturbations (2/2)

Considering a flat wCDM background with $\Omega_{\mathrm{r},0} = 0$, the Hubble rate is

$$H^2(a) = H_0^2 \left[\Omega_{\mathrm{m},0}\, a^{-3} + (1 - \Omega_{\mathrm{m},0})\, a^{-3(1+w)}\right] \tag{4}$$

and thus we can solve numerically the dynamical growth equation

$$\delta''(a) + \left(\frac{3}{a} + \frac{H'(a)}{H(a)}\right)\delta'(a) - \frac{3}{2}\frac{\Omega_{\mathrm{m},0}\, G_{\mathrm{eff}}(a,k)/G_{\mathrm{N}}}{a^5 H^2(a)/H_0^2}\, \delta(a) = 0 \tag{5}$$

and construct the theoretically predicted $f\sigma_8$ as

$$f\sigma_8(a) \equiv f(a)\cdot\sigma(a) = \frac{\sigma_8}{\delta(1)}\, a\, \delta'(a) \tag{6}$$

Growth Data: Observational Probe of Perturbations (2/2)

Considering a flat wCDM background with $\Omega_{\mathrm{r},0} = 0$, the Hubble rate is

$$H^2(a) = H_0^2 \left[\Omega_{\mathrm{m},0}\, a^{-3} + (1 - \Omega_{\mathrm{m},0})\, a^{-3(1+w)}\right] \tag{4}$$

and thus we can solve numerically the dynamical growth equation

$$\delta''(a) + \left(\frac{3}{a} + \frac{H'(a)}{H(a)}\right)\delta'(a) - \frac{3}{2}\frac{\Omega_{\mathrm{m},0}\, G_{\mathrm{eff}}(a,k)/G_{\mathrm{N}}}{a^5 H^2(a)/H_0^2}\ \delta(a) = 0 \tag{5}$$

and construct the theoretically predicted $f\sigma_8$ as

$$f\sigma_8(a) \equiv f(a)\cdot\sigma(a) = \frac{\sigma_8}{\delta(1)}\ a\ \delta'(a) \tag{6}$$

In the analysis of the first paper we consider the viable parametrization of the form

$$G_{\mathrm{eff}} = G_{\mathrm{N}}\left[1 + g_a(1-a)^n - g_a(1-a)^{n+m}\right] \tag{7}$$

where g_a is a phenomenological parameter and n, m correspond to integer parameters with $n \geq 2$ and $m > 0$. In the analysis we set $n = m = 2$.

L. Kazantzidis, L. Perivolaropoulos Phys.Rev. D 97 (2018) no.10, 103503,
S. Nesseris et al. Phys.Rev. D96 (2017) no.2, 023542

Model Predictions

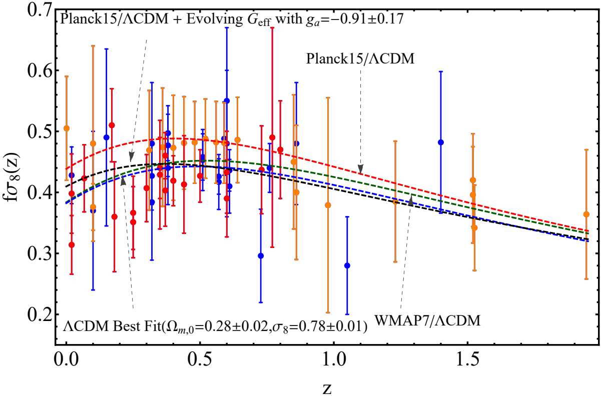

The Planck15/ΛCDM prediction (red dashed line) is higher than the majority of the $f\sigma_8$ datapoints indicating that the growth rate is too large. The fit improves either by considering a smaller value of $\Omega_{\rm m,0}$ and/or σ_8 (*e.g.* considering the results of the survey WMAP7 - green dashed line) or by adopting an evolving parametrization with $G_{\rm eff} < G_{\rm N}$ at low z, *i.e.* similar to the previous one for $g_\alpha < 0$ (black dashed line).

χ^2 Formation (1/2)

- We define the vector

$$V^i(z_i, \Omega_{\mathrm{m},0}, g_a, \sigma_8) \equiv f\sigma_{8,i} - \frac{f\sigma_8(z_i, \Omega_{\mathrm{m},0}, g_a, \sigma_8, g_a)}{q\left(z, \Omega_{\mathrm{m},0}, \Omega_{\mathrm{m},0}^{fid_i}\right)} \tag{8}$$

where $q(z, \Omega_{\mathrm{m},0}, \Omega'_{\mathrm{m},0})$ corresponds to the fiducial correction factor defined as

$$q(z, \Omega_{\mathrm{m},0}, \Omega'_{\mathrm{m},0}) = \frac{H(z)\, d_A(z)}{H'(z)\, d'_A(z)} \tag{9}$$

χ^2 Formation (1/2)

- We define the vector

$$V^i(z_i, \Omega_{\mathrm{m},0}, g_a, \sigma_8) \equiv f\sigma_{8,i} - \frac{f\sigma_8(z_i, \Omega_{\mathrm{m},0}, g_a, \sigma_8, g_a)}{q\left(z, \Omega_{\mathrm{m},0}, \Omega_{\mathrm{m},0}^{fid_i}\right)} \tag{8}$$

where $q(z, \Omega_{\mathrm{m},0}, \Omega'_{\mathrm{m},0})$ corresponds to the fiducial correction factor defined as

$$q(z, \Omega_{\mathrm{m},0}, \Omega'_{\mathrm{m},0}) = \frac{H(z)\, d_A(z)}{H'(z)\, d'_A(z)} \tag{9}$$

- The χ^2 function is constructed the usual way

$$\chi^2(\Omega_{\mathrm{m},0}, w, g_a, \sigma_8) = V^i C_{ij}^{-1} V^j \tag{10}$$

where C_{ij} is the total covariance matrix. C_{ij} is assumed to be diagonal except for the subset of WiggleZ survey (the only one published).

L. Kazantzidis, L. Perivolaropoulos Phys.Rev. D 97 (2018) no.10, 103503,
S. Nesseris et al. Phys.Rev. D96 (2017) no.2, 023542

χ^2 Formation (2/2)

The considered form of C_{ij} is

$$C_{ij}^{\text{growth,total}} = \begin{pmatrix} \sigma_1^2 & 0 & 0 & \cdots \\ 0 & C_{ij}^{WiggleZ} & 0 & \cdots \\ 0 & 0 & \cdots & \sigma_N^2 \end{pmatrix} \tag{11}$$

where $C_{ij}^{\text{WiggleZ}} = 10^{-3} \begin{pmatrix} 6.400 & 2.570 & 0.000 \\ 2.570 & 3.969 & 2.540 \\ 0.000 & 2.540 & 5.184 \end{pmatrix}$ and its non diagonal elements can be approximated as $C_{ij} \simeq 0.5\sqrt{C_{ii}C_{jj}}$. Obviously, this form is an oversestimation as it ignores the existing correlations among different datapoints.

L. Kazantzidis, L. Perivolaropoulos Phys.Rev. D 97 (2018) no.10, 103503,
S. Nesseris et al. Phys.Rev. D96 (2017) no.2, 023542

Growth Data Compilation ($f\sigma_{8,i}$) of our Analysis

z	$f\sigma_8 \pm \sigma_{f\sigma_8}$
0.35	0.440 ± 0.050
0.77	0.490 ± 0.18
0.17	0.510 ± 0.060
0.02	0.314 ± 0.048
0.02	0.398 ± 0.065
0.25	0.3512 ± 0.0583
0.37	0.4602 ± 0.0378
0.25	0.3665 ± 0.0601
0.37	0.4031 ± 0.0586
0.44	0.413 ± 0.080
0.60	0.390 ± 0.063
0.73	0.437 ± 0.072
0.067	0.423 ± 0.055
0.30	0.407 ± 0.055
0.40	0.419 ± 0.041
0.50	0.427 ± 0.043
0.60	0.433 ± 0.067
0.80	0.470 ± 0.080
0.35	0.429 ± 0.089
0.18	0.360 ± 0.090
0.38	0.440 ± 0.060
0.32	0.384 ± 0.095
0.32	0.48 ± 0.10
0.57	0.417 ± 0.045
0.15	0.490 ± 0.145
0.10	0.370 ± 0.130
1.40	0.482 ± 0.116
0.59	0.488 ± 0.060
0.38	0.497 ± 0.045
0.51	0.458 ± 0.038
0.61	0.436 ± 0.034
0.38	0.477 ± 0.051
0.51	0.453 ± 0.050
0.61	0.410 ± 0.044
0.76	0.440 ± 0.040
1.05	0.280 ± 0.080
0.32	0.427 ± 0.056
0.57	0.426 ± 0.029
0.727	0.296 ± 0.0765
0.02	0.428 ± 0.0465
0.6	0.48 ± 0.12
0.86	0.48 ± 0.10
0.60	0.550 ± 0.120
0.86	0.400 ± 0.110
0.1	0.48 ± 0.16
0.001	0.505 ± 0.085
0.85	0.45 ± 0.11
0.31	0.469 ± 0.098
0.36	0.474 ± 0.097
0.40	0.473 ± 0.086
0.44	0.481 ± 0.076
0.48	0.482 ± 0.067
0.52	0.488 ± 0.065
0.56	0.482 ± 0.067
0.59	0.481 ± 0.066
0.64	0.486 ± 0.070
0.1	0.376 ± 0.038
1.52	0.420 ± 0.076
0.978	0.379 ± 0.176
1.23	0.385 ± 0.099
1.526	0.342 ± 0.070
1.944	0.364 ± 0.106

The $1\sigma - 4\sigma$ Confidence Contours

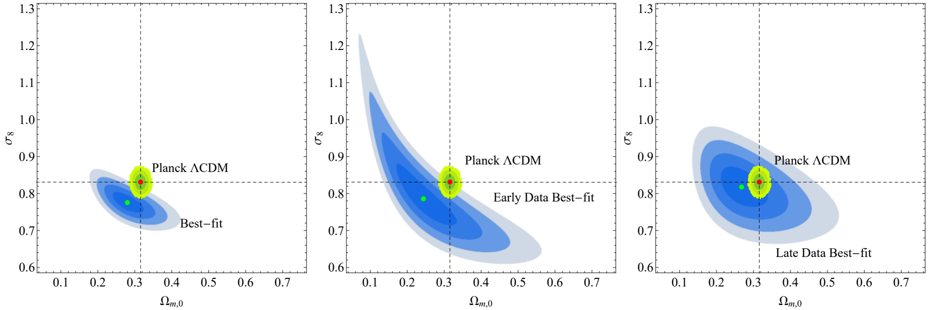

	Full Dataset Tension	Early Data Tension	Late Data Tension
$\Omega_{\mathrm{m},0} - \sigma_8$ Contours	4.97σ	3.89σ	0.94σ

The $1\sigma - 4\sigma$ Confidence Contours

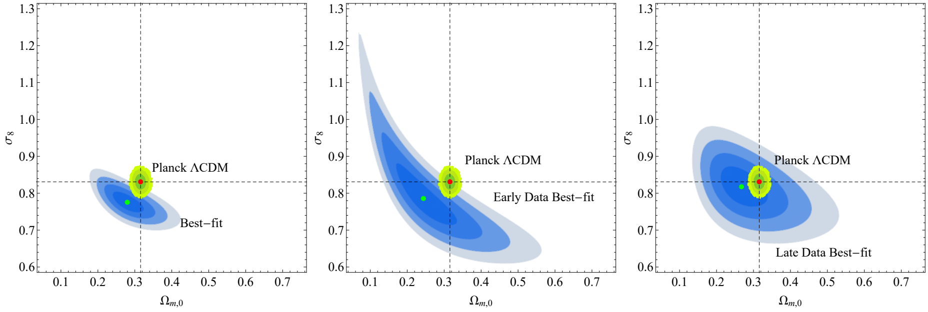

	Full Dataset Tension	Early Data Tension	Late Data Tension
$\Omega_{\mathrm{m},0} - \sigma_8$ Contours	4.97σ	3.89σ	0.94σ

General Trend: The tension disappears (becomes less than 1σ) when a subsample of the 20 most recently published data is used.

Reasons for the Evolution of the Tension

This general trend can be due to the following

(i) The fiducial models considered in early datapoints that were different from the Planck15/ΛCDM considered in more recent studies.

Reasons for the Evolution of the Tension

This general trend can be due to the following

(i) The fiducial models considered in early datapoints that were different from the Planck15/ΛCDM considered in more recent studies.

(ii) The assumed form of the covariance matrix.

Reasons for the Evolution of the Tension

This general trend can be due to the following

(i) The fiducial models considered in early datapoints that were different from the Planck15/ΛCDM considered in more recent studies.

(ii) The assumed form of the covariance matrix.

(iii) The increased redshifts of more recent datapoints.

Reasons for the Evolution of the Tension

This general trend can be due to the following

(i) The fiducial models considered in early datapoints that were different from the Planck15/ΛCDM considered in more recent studies.

(ii) The assumed form of the covariance matrix.

(iii) The increased redshifts of more recent datapoints.

(iv) Improved methods and reduced systematics.

Reasons for the Evolution of the Tension

This general trend can be due to the following

(i) The fiducial models considered in early datapoints that were different from the Planck15/ΛCDM considered in more recent studies.

(ii) The assumed form of the covariance matrix.

(iii) The increased redshifts of more recent datapoints.

(iv) Improved methods and reduced systematics.

i) Fiducial Model Correction

Recall that the correction factor $q(z, \Omega_{\mathrm{m},0}, \Omega'_{\mathrm{m},0})$ that we used in the analysis should be taken as a rough estimate and is of the form

$$q(z, \Omega_{\mathrm{m},0}, \Omega'_{\mathrm{m},0}) = [H(z)\, d_A(z)]/[H'(z)\, d'_A(z)] \tag{12}$$

so, in order to estimate its effect, we set $q = 1$ and re-construct the confidence contours in the same parametric space

i) Fiducial Model Correction

Recall that the correction factor $q(z, \Omega_{\rm m,0}, \Omega'_{\rm m,0})$ that we used in the analysis should be taken as a rough estimate and is of the form

$$q(z, \Omega_{\rm m,0}, \Omega'_{\rm m,0}) = [H(z)\, d_A(z)]/[H'(z)\, d'_A(z)] \tag{12}$$

so, in order to estimate its effect, we set $q = 1$ and reconstruct the confidence contours in the same parametric space

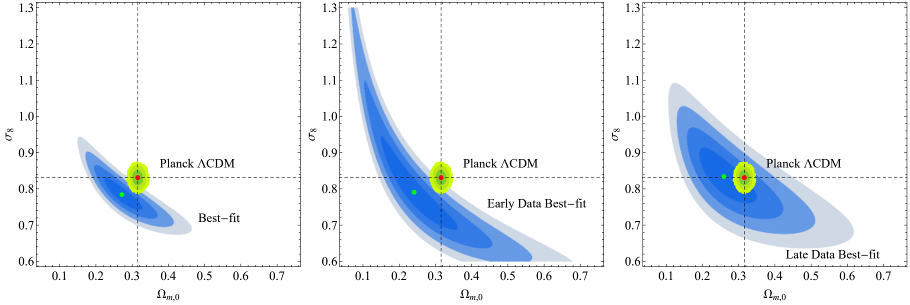

i) Fiducial Model Correction

Recall that the correction factor $q(z, \Omega_{\rm m,0}, \Omega'_{\rm m,0})$ that we used in the analysis should be taken as a rough estimate and is of the form

$$q(z, \Omega_{\rm m,0}, \Omega'_{\rm m,0}) = [H(z)\, d_A(z)]/[H'(z)\, d'_A(z)] \tag{12}$$

so, in order to estimate its effect, we set $q = 1$ and re-construct the confidence contours in the same parametric space

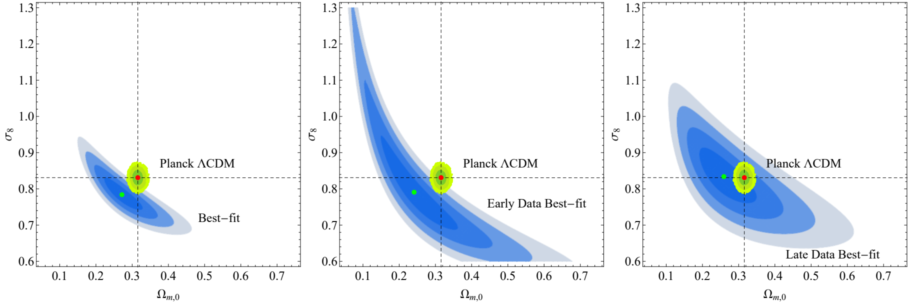

Result: The qualitative feature of the reduced tension for late data remains practically unaffected.

ii) Form of the Total Covariance Matrix

- We introduce a number of randomly selected non-diagonal elements and apply positive correlations in 12 randomly selected pairs of datapoints (about 20% of the data) while keeping the total covariance matrix symmetric.

ii) Form of the Total Covariance Matrix

- We introduce a number of randomly selected non-diagonal elements and apply positive correlations in 12 randomly selected pairs of datapoints (about 20% of the data) while keeping the total covariance matrix symmetric.
- The positions of the non-diagonal elements are chosen randomly and the magnitude of the randomly selected covariance matrix element C_{ij} is set to be $C_{ij} = (1/2)\,\sigma_i\,\sigma_j$

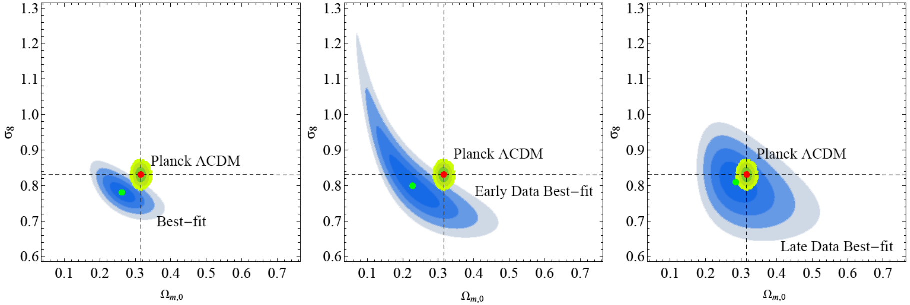

ii) Form of the Total Covariance Matrix

- We introduce a number of randomly selected non-diagonal elements and apply positive correlations in 12 randomly selected pairs of datapoints (about 20% of the data) while keeping the total covariance matrix symmetric.
- The positions of the non-diagonal elements are chosen randomly and the magnitude of the randomly selected covariance matrix element C_{ij} is set to be $C_{ij} = (1/2)\,\sigma_i\,\sigma_j$

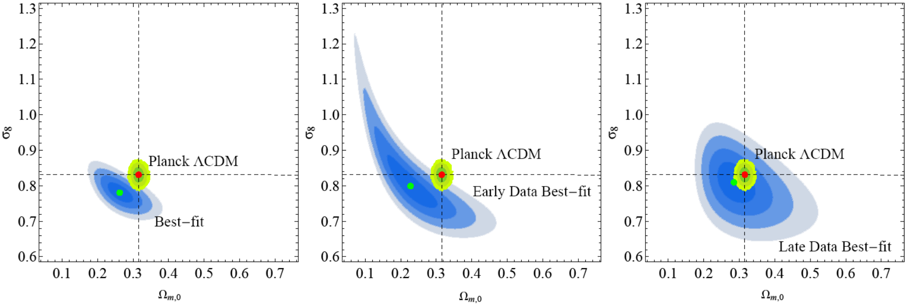

Result: The introduction of a nontrivial covariance matrix does not change the qualitative conclusion of the reduced tension.

iii) Increased Redshifts of More Recent Datapoints

- The trend for reduced tension of the growth data with Planck15/ΛCDM can be due to the increased redshifts of more recent datapoints.

iii) Increased Redshifts of More Recent Datapoints

- The trend for reduced tension of the growth data with Planck15/ΛCDM can be due to the increased redshifts of more recent datapoints.
- Due to the probe of higher redshifts the more recent datapoints also have larger errorbars.

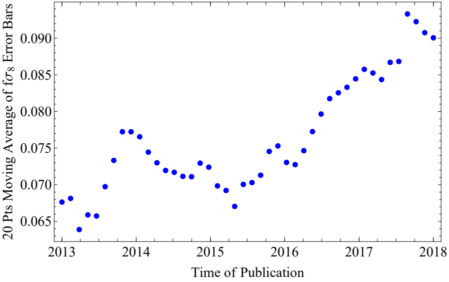

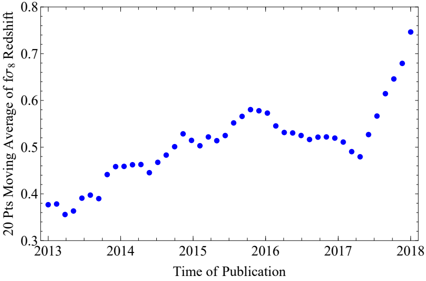

iii) Increased Redshifts of More Recent Datapoints

- The trend for reduced tension of the growth data with Planck15/ΛCDM can be due to the increased redshifts of more recent datapoints.
- Due to the probe of higher redshifts the more recent datapoints also have larger errorbars.

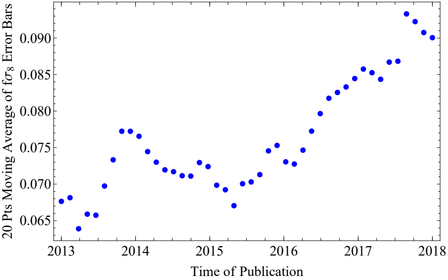

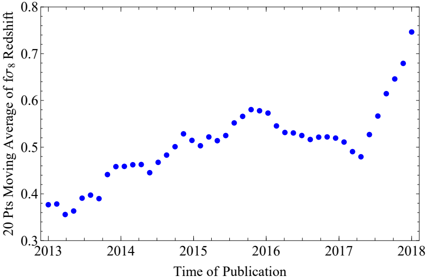

Result: More recent datapoints probe redshift regions where different ΛCDM models make similar predictions. This degeneracy is due to matter domination that appears in all viable models at early times.

Parameter g_α

- The trend for reduced tension of recent growth data with Planck15/ΛCDM implies also a trend for reduced indications in the parameter g_α.

Parameter g_α

- The trend for reduced tension of recent growth data with Planck15/ΛCDM implies also a trend for reduced indications in the parameter g_α.
- The 1σ range implied for g_α from the full $f\sigma_8$ data set (red point), and for 20 point $f\sigma_8$ subsamples starting from the earliest to the latest subsample

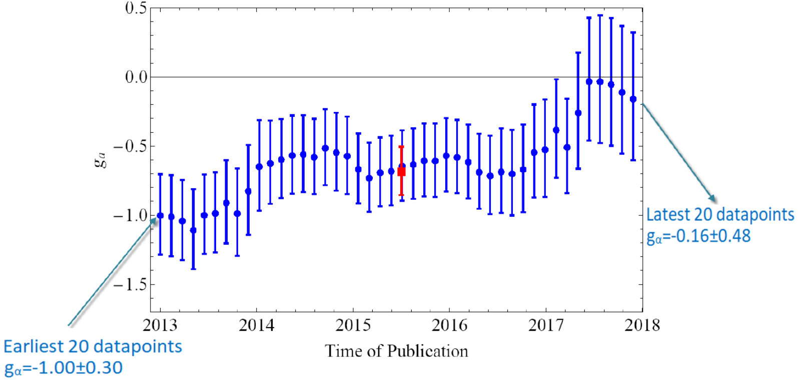

Result: Only late data are consistent with GR.

Consistency with $f(R)$ Theories

- The best fit form of the parameter g_α indicate a decreasing $G_{\rm eff}(z)$ at low z which may lead to constraints on the fundamental parameters of modified theories of gravity.
- The basic question that arises is the following "Which modified gravity models are consistent with $\frac{G_{\rm eff}(z)}{G_{\rm N}} < 1$ at low z?"

Consistency with $f(R)$ Theories

- The best fit form of the parameter g_α indicate a decreasing $G_{\rm eff}(z)$ at low z which may lead to constraints on the fundamental parameters of modified theories of gravity.
- The basic question that arises is the following "Which modified gravity models are consistent with $\frac{G_{\rm eff}(z)}{G_{\rm N}} < 1$ at low z?"
- For viable $f(R)$ theories the answer is clearly negative since

$$G_{\rm eff}(k,z) = G_{\rm N}\left\{\left(\frac{df}{dR}\right)^{-1}\left[\frac{1+4\left(\frac{d^2f}{dR^2}/\frac{df}{dR}\right)\cdot k^2(1+z)^2}{1+3\left(\frac{d^2f}{dR^2}/\frac{df}{dR}\right)\cdot k^2(1+z)^2}\right]\right\} \tag{13}$$

which lead to $\frac{G_{\rm eff}(z)}{G_{\rm N}} > 1$ since the factor in front of the brackets in (13) increases when R decreases with the expansion, and thus it is always larger than one. Hence, the $f(R)$ modified gravity theories are inconsistent with the trend indicated by growth data, independently of the form of the background $H(z)$.

A. Starobinsky JETP Lett. 86, 157163 (2007),
R. Gannouji, L. Kazantzidis, D. Polarski, L. Perivolaropoulos Phys.Rev. D 98 (2018) no.10, 104044

Consistency with Scalar Tensor Theories (1/3)

- In scalar-tensor gravity the action has the following form

$$S = \int d^4x\sqrt{-g}\left[\frac{1}{2}F(\phi)R - \frac{1}{2}g^{\mu\nu}\partial_\mu\phi\partial_\nu\phi - U(\phi)\right] + S_m \qquad (14)$$

Consistency with Scalar Tensor Theories (1/3)

- In scalar-tensor gravity the action has the following form

$$S = \int d^4x\sqrt{-g}\left[\frac{1}{2}F(\phi)R - \frac{1}{2}g^{\mu\nu}\partial_\mu\phi\partial_\nu\phi - U(\phi)\right] + S_m \tag{14}$$

- By varying this action we get the corresponding equations of motion. Usually it is convenient to express the equations in terms of the redshift z. So in scalar tensor theories the Newton's constant present a dynamical evolution and is of the form

$$G_{\mathrm{eff}}(z)/G_{\mathrm{N}} = \frac{1}{F(z)}\frac{F(z) + 2F_{,\phi}^2}{F(z) + \frac{3}{2}F_{,\phi}^2} \tag{15}$$

Consistency with Scalar Tensor Theories (1/3)

- In scalar-tensor gravity the action has the following form

$$S = \int d^4x \sqrt{-g} \left[\frac{1}{2} F(\phi) R - \frac{1}{2} g^{\mu\nu} \partial_\mu \phi \partial_\nu \phi - U(\phi) \right] + S_m \tag{14}$$

- By varying this action we get the corresponding equations of motion. Usually it is convenient to express the equations in terms of the redshift z. So in scalar tensor theories the Newton's constant present a dynamical evolution and is of the form

$$G_{\mathrm{eff}}(z)/G_{\mathrm{N}} = \frac{1}{F(z)} \frac{F(z) + 2F_{,\phi}^2}{F(z) + \frac{3}{2} F_{,\phi}^2} \tag{15}$$

- For low z we can expand the dynamical Newton's constant $G_{\mathrm{eff}}(z)$, which up to the second order is of the following form

$$G_{\mathrm{eff}}(z) = G_{\mathrm{eff}}(0) + G'_{\mathrm{eff}}(0) z + \frac{z^2}{2} G''_{\mathrm{eff}}(0) + \ldots \tag{16}$$

G. Esposito-Farese and D. Polarski Phys. Rev. D 63 (2001) 063504
R. Gannouji, L. Kazantzidis, D. Polarski, L. Perivolaropoulos Phys.Rev. D 98 (2018) no.10, 104044

Consistency with Scalar Tensor Theories (2/3)

- Applying the solar system constraints, i.e. that

$$\lim_{z\to 0} G'_{\mathrm{eff}}(z) \simeq 0$$

we deduce that Eq. (16) reduces to

$$G_{\mathrm{eff}}(z) = G_{\mathrm{eff}}(0) + \frac{z^2}{2} G''_{\mathrm{eff}}(0) + \ldots \tag{17}$$

Consistency with Scalar Tensor Theories (2/3)

- Applying the solar system constraints, i.e. that

$$\lim_{z\to 0} G'_{\rm eff}(z) \simeq 0$$

we deduce that Eq. (16) reduces to

$$G_{\rm eff}(z) = G_{\rm eff}(0) + \frac{z^2}{2} G''_{\rm eff}(0) + \dots \tag{17}$$

- Furthermore at $z = 0$ we have, $G'_{\rm eff}(0) = 0 \to F'(0) = 0$ and that $G_{\rm eff}(0) = G_{\rm N} = 1 \to F(0) = 1$ so we obtain

$$G''_{\rm eff}(0) = F''(0)\left(-1 + \frac{F''(0)}{\phi'(0)^2}\right)$$

Assuming once again a wCDM background, the second derivative of $G_{\rm eff}(z)$ at $z = 0$ takes the following form

$$G''_{\rm eff}(0) = 9(1+w)(-1+\Omega_{\rm m,0}) + \frac{9(1+w)^2(-1+\Omega_{\rm m,0})^2}{\phi'(0)^2} + 2\,\phi'(0)^2 \tag{18}$$

S. Nesseris and L. Perivolaropoulos, Phys. Rev. D75 (2007) 023517
R. Gannouji, L. Kazantzidis, D. Polarski, L. Perivolaropoulos Phys.Rev. D 98 (2018) no.10, 104044

Consistency with Scalar Tensor Theories (3/3)

Fixing a ΛCDM background in Eq. (18), then Eq. (17) takes the form

$$G_{\mathrm{eff}}(z) = G_{\mathrm{eff}}(0) + \frac{1}{2} G''_{\mathrm{eff}}(0)\, z^2 = G_{\mathrm{N}} + \frac{1}{2} G''_{\mathrm{eff}}(0)\, z^2 = 1 + \phi'(0)^2\, z^2 + \ldots \tag{19}$$

which is always an increasing function of z if we assume that the kinetic term of $\phi'(z)$ is always positive, an assumption crucial for a self-consistent theory. This is also demonstrated in the figure below

Consistency with Scalar Tensor Theories (3/3)

Fixing a ΛCDM background in Eq. (18), then Eq. (17) takes the form

$$G_{\rm eff}(z) = G_{\rm eff}(0) + \frac{1}{2} G''_{\rm eff}(0)\, z^2 = G_{\rm N} + \frac{1}{2} G''_{\rm eff}(0)\, z^2 = 1 + \phi'(0)^2\, z^2 + \ldots \tag{19}$$

which is always an increasing function of z if we assume that the kinetic term of $\phi'(z)$ is always positive, an assumption crucial for a self-consistent theory. This is also demonstrated in the figure below

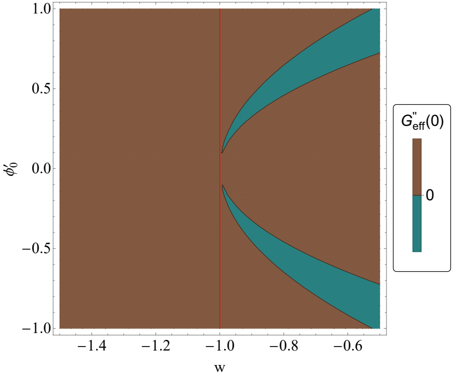

R. Gannouji, L. Kazantzidis, D. Polarski, L. Perivolaropoulos Phys.Rev. D 98 (2018) no.10, 104044

MGCAMB Results

- If the Newton's constant is indeed evolving with redshift, then we expect to find similar hints to other geometrical and/or dynamical probes, such as the CMB and the SnIa data. An evolving $G_{\rm eff}(z)$ would affect the low l CMB angular power spectrum due to the Integrated Sachs Wolfe effect.
- To quantify this effect, we reconstruct the CMB power spectrum using the 2019 version of the Modified Growth with CAMB (MGCAMB) numerical package

MGCAMB Results

- If the Newton's constant is indeed evolving with redshift, then we expect to find similar hints to other geometrical and/or dynamical probes, such as the CMB and the SnIa data. An evolving $G_{\rm eff}(z)$ would affect the low l CMB angular power spectrum due to the Integrated Sachs Wolfe effect.
- To quantify this effect, we reconstruct the CMB power spectrum using the 2019 version of the Modified Growth with CAMB (MGCAMB) numerical package

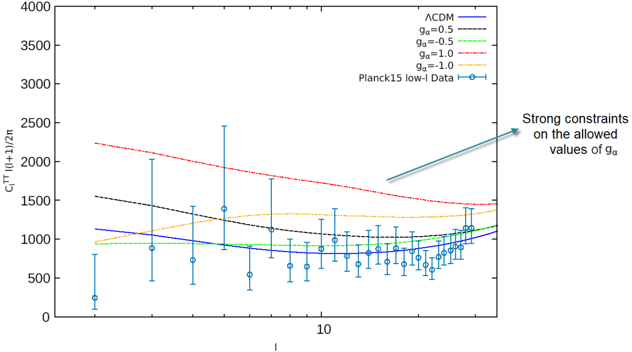

L. Perivolaropoulos and L. Kazantzidis, Book Chapter In: Saridakis E.N. et al. (eds) Modified Gravity and Cosmology. Springer

MGCOSMOMC Results

In order to fully constrain the values of the predicted observables we use the 2019 version of Modified Growth with Cosmological MonteCarlo (MGCOSMOMC) fixing the majority of the parameters to the corresponding Planck15/ΛCDM values and derive the following $1\sigma - 2\sigma$ confidence contours

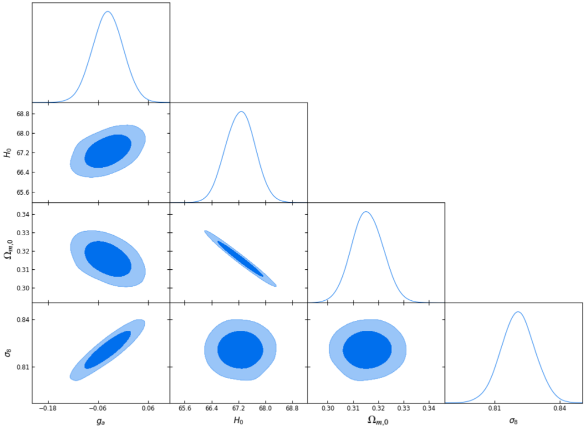

L. Perivolaropoulos and L. Kazantzidis, Book Chapter In: Saridakis E.N. et al. (eds) Modified Gravity and Cosmology. Springer

$M - H_0$ Degeneracy

- An evolving $G_{\mathrm{eff}}(z)$ would leave a characteristic signature in SnIa data, since it implies an evolving Chandrasekhar mass m_{ch} leading to lower values for the absolute magnitude M at recent cosmological times with respect to the best fit value of M in the context of ΛCDM.

$M - H_0$ Degeneracy

- An evolving $G_{\mathrm{eff}}(z)$ would leave a characteristic signature in SnIa data, since it implies an evolving Chandrasekhar mass m_{ch} leading to lower values for the absolute magnitude M at recent cosmological times with respect to the best fit value of M in the context of ΛCDM.
- However, the absolute magnitude M is degenerate with H_0 through the parameter $\mathcal{M}$ (usually marginalized as a nuisance parameter) that is defined as

$$\mathcal{M} \equiv M + 5\, log_{10}\left(\frac{c/H_0}{1Mpc}\right) + 25 = M - 5\, log_{10}(h) + 42.38 \tag{20}$$

where $h \equiv H_0/100\ km\, s^{-1}\, Mpc^{-1}$, leading to lower values of $\mathcal{M}$ at low z than the standard ΛCDM ones.

$M - H_0$ Degeneracy

- An evolving $G_{\rm eff}(z)$ would leave a characteristic signature in SnIa data, since it implies an evolving Chandrasekhar mass m_{ch} leading to lower values for the absolute magnitude M at recent cosmological times with respect to the best fit value of M in the context of ΛCDM.
- However, the absolute magnitude M is degenerate with H_0 through the parameter $\mathcal{M}$ (usually marginalized as a nuisance parameter) that is defined as

$$\mathcal{M} \equiv M + 5\, log_{10}\left(\frac{c/H_0}{1Mpc}\right) + 25 = M - 5\, log_{10}(h) + 42.38 \qquad (20)$$

  where $h \equiv H_0/100\ km\, s^{-1}\ Mpc^{-1}$, leading to lower values of $\mathcal{M}$ at low z than the standard ΛCDM ones.
- Such an effect could be also caused by higher local values of H_0 in the context of *e.g.* a local matter underdensity scenario.

SnIa as Standard Candles

- SnIa have been widely used as standard candles to probe the expansion rate $H(z)$ of the late Universe. The theoretically predicted apparent magnitude $m_{th}(z)$ of the SnIa can be expressed as

$$m_{th}(z) = M + 5\,log_{10}\left[D_L(z)\right] + 5\,log_{10}\left(\frac{c/H_0}{1Mpc}\right) + 25 = \mathcal{M} + 5\,log_{10}\left[D_L(z)\right] \tag{21}$$

where $D_L(z) \equiv H_0\, d_L(z)/c$ is the Hubble free luminosity distance and the luminosity distance $d_L(z)$ in a flat Universe is

$$d_L(z) = c\,(1+z)\int_0^z \frac{dz'}{H(z')} \tag{22}$$

SnIa as Standard Candles

- SnIa have been widely used as standard candles to probe the expansion rate $H(z)$ of the late Universe. The theoretically predicted apparent magnitude $m_{th}(z)$ of the SnIa can be expressed as

$$m_{th}(z) = M + 5\, log_{10}\left[D_L(z)\right] + 5\, log_{10}\left(\frac{c/H_0}{1Mpc}\right) + 25 = \mathcal{M} + 5\, log_{10}\left[D_L(z)\right] \tag{21}$$

where $D_L(z) \equiv H_0\, d_L(z)/c$ is the Hubble free luminosity distance and the luminosity distance $d_L(z)$ in a flat Universe is

$$d_L(z) = c\,(1+z)\int_0^z \frac{dz'}{H(z')} \tag{22}$$

- The latest publicly available that is the Pantheon dataset consisting of six independent probes that cover the redshift range $0.01 < z < 2.3$, giving a total of 1048 SnIa. The relevant χ^2 function is

$$\chi^2(\mathcal{M},\Omega_{\mathrm{m},0}) = V^i_{Panth.}\, \bar{C}^{-1}_{ij}\, V^j_{Panth.} \tag{23}$$

where $V^i_{Panth.} \equiv m_{obs}(z_i) - m_{th}(z)$ and $\bar{C}_{ij}$ is the diagonal covariance matrix of the statistical uncertainties.

Pantheon Results (1/4)

- Applying the maximum likelihood method for a ΛCDM background, we get $\Omega_{\mathrm{m},0} = 0.285 \pm 0.012$ and $\mathcal{M} = 23.803 \pm 0.007$. For a redshift independent $\mathcal{M}$, we anticipate that any subset of the Pantheon dataset should give a best fit value consistent (within the 1σ threshold) with the corresponding best fit values of the full dataset.

Pantheon Results (1/4)

- Applying the maximum likelihood method for a ΛCDM background, we get $\Omega_{\mathrm{m},0} = 0.285 \pm 0.012$ and $\mathcal{M} = 23.803 \pm 0.007$. For a redshift independent $\mathcal{M}$, we anticipate that any subset of the Pantheon dataset should give a best fit value consistent (within the 1σ threshold) with the corresponding best fit values of the full dataset.
- We use two different methods to test this hypothesis:
  - We consider cumulative subsets of the full data compilation with redshift ranges $z \in [0.02, z_{max}]$, where z_{max} is a cutoff redshift increasing in steps of $\Delta z_{max} = 0.01$ and apply the maximum likelihood method for each subset.

Pantheon Results (1/4)

- Applying the maximum likelihood method for a ΛCDM background, we get $\Omega_{\mathrm{m},0} = 0.285 \pm 0.012$ and $\mathcal{M} = 23.803 \pm 0.007$. For a redshift independent $\mathcal{M}$, we anticipate that any subset of the Pantheon dataset should give a best fit value consistent (within the 1σ threshold) with the corresponding best fit values of the full dataset.
- We use two different methods to test this hypothesis:
  - We consider cumulative subsets of the full data compilation with redshift ranges $z \in [0.02, z_{max}]$, where z_{max} is a cutoff redshift increasing in steps of $\Delta z_{max} = 0.01$ and apply the maximum likelihood method for each subset.
  - We consider cumulative bins by ranking the Pantheon data from lower to higher redshifts finding the best fit value of $\mathcal{M}$ along with the corresponding 1σ error in the context of ΛCDM for the first 100 points and repeating the above procedure for the entire dataset (the i^{th} point is obtained by repeating the above procedure for the datapoints from i to $i + 100$).

L. Kazantzidis and L. Perivolaropoulos Phys.Rev.D 101 (2020) 12, 123516

Pantheon Results (2/4)

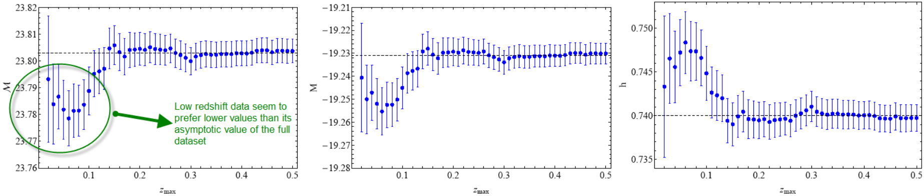

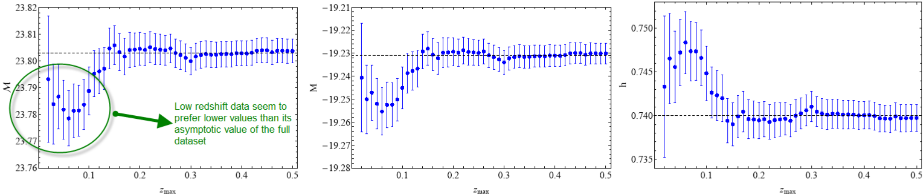

Result: At low reshifts and in particular in the resdhift range $z_{max} \in [0.02, 0.15]$ the data seem to prefer lower values of $\mathcal{M}$ from the best fit value indicated by the full dataset (continuous dashed line). This difference is at a level of about 2σ and drops drastically for $z_{max} > 0.15$. The observed difference in the resdhift range $z_{max} \in [0.02, 0.15]$, corresponds to lower values of M (middle panel) or equivalently higher values of h (right panel).

L. Kazantzidis and L. Perivolaropoulos Phys.Rev.D 101 (2020) 12, 123516

Pantheon Results (3/4)

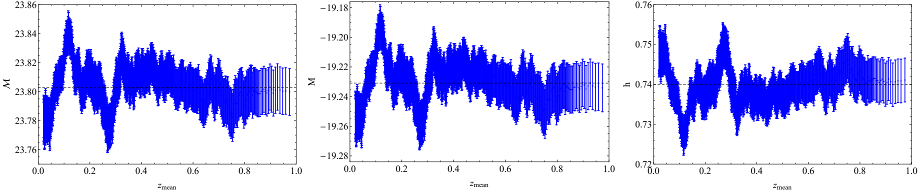

Pantheon Results (3/4)

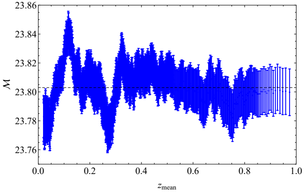

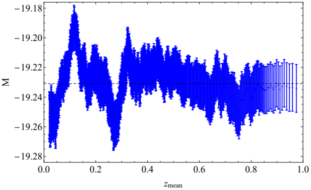

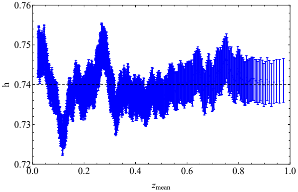

Result: For $z_{mean} < 0.3$ the best fit value of $\mathcal{M}$ oscillates around the best fit value of the full dataset at a level of about $1\sigma - 2\sigma$ implying a similar behavior for M (middle panel) and h (right panel) in the same redshift range. The redshift range of the oscillation in this case is larger than the detected redshift range of the variation since as the cutoff redshift increases, so does the size of the corresponding subsample canceling as a result the oscillating effect.

L. Kazantzidis and L. Perivolaropoulos Phys.Rev.D 101 (2020) 12, 123516

Pantheon Results (4/4)

In order to increase the low z subsample and improve the statistics, we sort once more the Pantheon data from lowest to highest redshifts and split the entire dataset in foul equal bins containing 262 uncorrelated datapoints.

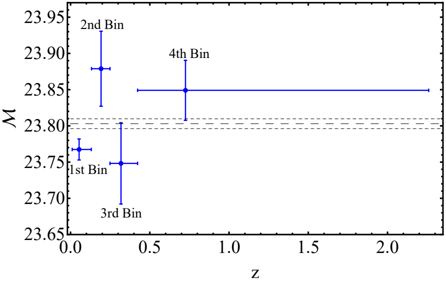

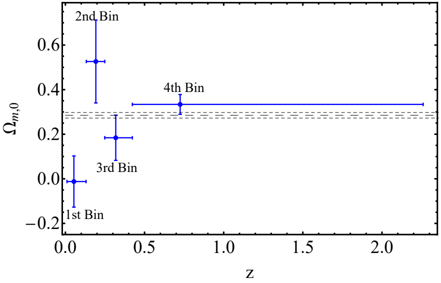

Pantheon Results (4/4)

In order to increase the low z subsample and improve the statistics, we sort once more the Pantheon data from lowest to highest redshifts and split the entire dataset in foul equal bins containing 262 uncorrelated datapoints.

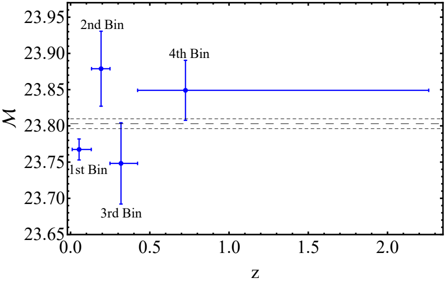

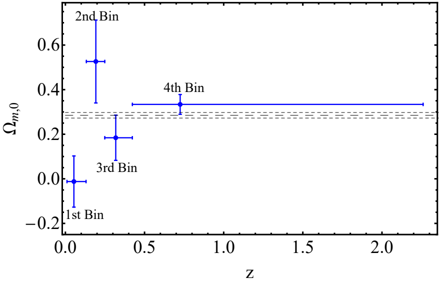

Result: An oscillating behaviour such as the previous one is evident at low redshifts z. Notice that the best fit values of $\mathcal{M}$ and $\Omega_{\mathrm{m},0}$ for the lowest z bin $(0.01 < z < 0.13)$ are more than 2σ lower than the corresponding best fit values of the full dataset. For the first bin we derive $\Delta\mathcal{M} \equiv \mathcal{M}_{bf} - \mathcal{M}_{bin1} \approx 0.04 \pm 0.02$ $\rightarrow \delta\rho_0/\rho_0 = -0.10 \pm 0.04$

L. Kazantzidis and L. Perivolaropoulos Phys.Rev.D 101 (2020) 12, 123516

Possible Explanations

The $\approx 2\sigma$ detected signal regarding $\mathcal{M}$ at low redshifts can be attributed

(i) A local underdensity that vanishes at large scales, since a lower $\mathcal{M}$ than the best fit value indicated by the full dataset in the low redshift regime, leads to a higher value of h. $\rightarrow$ Not Excluded by the Pantheon Data.

Possible Explanations

The $\approx 2\sigma$ detected signal regarding $\mathcal{M}$ at low redshifts can be attributed

(i) A local underdensity that vanishes at large scales, since a lower $\mathcal{M}$ than the best fit value indicated by the full dataset in the low redshift regime, leads to a higher value of h. $\rightarrow$ Not Excluded by the Pantheon Data.

(ii) A modified theory of gravity, since it implies a redshift depence of the absolute magnitude M, due to *e.g.* a time variation of Newton's constant in the context of a modified theory scenario. $\rightarrow$ Not Excluded by the Pantheon Data.

Possible Explanations

The $\approx 2\sigma$ detected signal regarding $\mathcal{M}$ at low redshifts can be attributed

(i) A local underdensity that vanishes at large scales, since a lower $\mathcal{M}$ than the best fit value indicated by the full dataset in the low redshift regime, leads to a higher value of h. $\rightarrow$ Not Excluded by the Pantheon Data.

(ii) A modified theory of gravity, since it implies a redshift depence of the absolute magnitude M, due to *e.g.* a time variation of Newton's constant in the context of a modified theory scenario. $\rightarrow$ Not Excluded by the Pantheon Data.

(iii) Statistical and/or systematic fluctuations of the data around the true ΛCDM model. The probability of this case can be estimated creating a large number of simulated Pantheon like datasets in the context of a ΛCDM background taking into account the full covariance matrix C_{ij}. $\rightarrow$ Not Excluded by the Pantheon Data.

H_0 Crisis or M Crisis? (1/2)

- The H_0 Tension refers to the incosistency between the measurement of the SnIa $H_0 = 73.04 \pm 1.04\ km\, s^{-1}\, Mpc^{-1}$ (standard distance ladder method) and the measurement from the CMB data $H_0 = 67.36 \pm 0.54\ km \cdot\ s^{-1} \cdot \cdot\ Mpc^{-1}$ (inverse distance ladder method).

H_0 Crisis or M Crisis? (1/2)

- The H_0 Tension refers to the incosistency between the measurement of the SnIa $H_0 = 73.04 \pm 1.04 \; km \, s^{-1} \, Mpc^{-1}$ (standard distance ladder method) and the measurement from the CMB data $H_0 = 67.36 \pm 0.54 \; km \cdot \; s^{-1} \cdot \cdot Mpc^{-1}$ (inverse distance ladder method).
- The basic steps of the standard distance ladder method are the following:
  - Calibrate the Cepheid variable stars applying parallax methods.
  - Use the calculated distances to "move further" towards galaxies that include mostly SnIa.

H_0 Crisis or M Crisis? (1/2)

- The H_0 Tension refers to the incosistency between the measurement of the SnIa $H_0 = 73.04 \pm 1.04\ km\, s^{-1}\, Mpc^{-1}$ (standard distance ladder method) and the measurement from the CMB data $H_0 = 67.36 \pm 0.54\ km \cdot\ s^{-1} \cdot$ $\cdot\ Mpc^{-1}$ (inverse distance ladder method).
- The basic steps of the standard distance ladder method are the following:
  - Calibrate the Cepheid variable stars applying parallax methods.
  - Use the calculated distances to "move further" towards galaxies that include mostly SnIa.
  - Using Eq. (21) [Eq. for $m_{th}(z)$] in the redshift range $0.023 < z < 0.15$, the parameter $\mathcal{M}$ is measured under the assumption of a constant $M \equiv M_c$.

H_0 Crisis or M Crisis? (1/2)

- The H_0 Tension refers to the incosistency between the measurement of the SnIa $H_0 = 73.04 \pm 1.04\ km\, s^{-1}\, Mpc^{-1}$ (standard distance ladder method) and the measurement from the CMB data $H_0 = 67.36 \pm 0.54\ km \cdot\ s^{-1} \cdot$ $\cdot\ Mpc^{-1}$ (inverse distance ladder method).
- The basic steps of the standard distance ladder method are the following:
  - Calibrate the Cepheid variable stars applying parallax methods.
  - Use the calculated distances to "move further" towards galaxies that include mostly SnIa.
  - Using Eq. (21) [Eq. for $m_{th}(z)$] in the redshift range $0.023 < z < 0.15$, the parameter $\mathcal{M}$ is measured under the assumption of a constant $M \equiv M_c$.
  - The considered Hubble free luminosity distance $D_L(z)$ is Taylor expanded as

$$D_L(z) = z\left[1 + \frac{1}{2}(1 - q_0)\, z - \frac{1}{6}(1 - q_0 - 3\, q_0^2 + j_0)\, z^2 + \dots\right]$$

    where $q_0 = -0.55$ and $j_0 = 1$ (ΛCDM values).
  - The value of H_0 is inferred using an extrapolation method.

A. G. Riess et al., Astrophys. J. 699, 539563 (2009)

H_0 Crisis or M Crisis? (2/2)

- This methodology, is oblivious to any possible transitions of M at $z < 0.023$. If for example, such a transition had occurred at $z_t = 0.01$ (or lower), then the M that was derived using the Cepheids for z up to ≈ 0.01 should not be considered to be the same for the nearby SnIa.

H_0 Crisis or M Crisis? (2/2)

- This methodology, is oblivious to any possible transitions of M at $z < 0.023$. If for example, such a transition had occurred at $z_t = 0.01$ (or lower), then the M that was derived using the Cepheids for z up to ≈ 0.01 should not be considered to be the same for the nearby SnIa.
- So, maybe the designation "M tension/crisis" might be more suitable to describe the problem.

H_0 Crisis or M Crisis? (2/2)

- This methodology, is oblivious to any possible transitions of M at $z < 0.023$. If for example, such a transition had occurred at $z_t = 0.01$ (or lower), then the M that was derived using the Cepheids for z up to ≈ 0.01 should not be considered to be the same for the nearby SnIa.
- So, maybe the designation "M tension/crisis" might be more suitable to describe the problem.
- We consider two dark energy models:
  - A dark energy model with a late time M transition model (LMT) of the form
  $$M(z) = M_< + \Delta M \, \Theta(z - z_t) \tag{24}$$
  where z_t corresponds to the transition redshift, $M_< \equiv M_c = -19.24$ mag is the Cepheid value, ΔM is the parameter that quantifies the shift from the M_c value and Θ corresponds to the Heaviside step function.

H_0 Crisis or M Crisis? (2/2)

- This methodology, is oblivious to any possible transitions of M at $z < 0.023$. If for example, such a transition had occurred at $z_t = 0.01$ (or lower), then the M that was derived using the Cepheids for z up to ≈ 0.01 should not be considered to be the same for the nearby SnIa.
- So, maybe the designation "M tension/crisis" might be more suitable to describe the problem.
- We consider two dark energy models:
  - A dark energy model with a late time M transition model (LMT) of the form
  $$M(z) = M_< + \Delta M \, \Theta(z - z_t) \tag{24}$$
  where z_t corresponds to the transition redshift, $M_< \equiv M_c = -19.24$ mag is the Cepheid value, ΔM is the parameter that quantifies the shift from the M_c value and Θ corresponds to the Heaviside step function.
  - A dark energy model with a late time M transition model including a simultaneous transition on the same redshift z_t of the dark energy w_{DE} ($LwMT$) of the form
  $$w_{DE}(z) = -1 + \Delta w \, \Theta(z_t - z) \tag{25}$$

Statistical Analysis Results (1/2)

- We modify the CLASS/MontePython numerical codes and consider the Planck18 CMB data (the TTTEEE likelihoods), the default BAO data as well as Lyα BAO data, the Pantheon SnIa compilation and a robust compilation of 18 RSD data.

Statistical Analysis Results (1/2)

- We modify the CLASS/MontePython numerical codes and consider the Planck18 CMB data (the TTTEEE likelihoods), the default BAO data as well as Lyα BAO data, the Pantheon SnIa compilation and a robust compilation of 18 RSD data.
- For the *LwMT* model we impose the priors $\Delta w \in [-0.7, 0.7]$ and $a_t \leq 0.99$ to obtain the following best fits

Parameter	best-fit	mean$\pm\sigma$	95.5% lower	95.5% upper
$\Omega_{m,0}$	0.3018	$0.3066^{+0.0064}_{-0.0065}$	0.2939	0.3196
H_0	68.56	$68.03^{+0.55}_{-0.58}$	66.94	69.15
σ_8	0.8141	0.8089 ± 0.0065	0.7957	0.8219
ΔM	-0.1676	-0.1698 ± 0.012	-0.1933	-0.1467
Δw	unconstrained	unconstrained	unconstrained	unconstrained
a_t	0.9856	> 0.985	> 0.984	> 0.984
$M_> \equiv M_c + \Delta M$	-19.408	-19.410 ± 0.012	-19.433	-19.387

$\chi^2_{\rm min}$	3834

Statistical Analysis Results (1/2)

- We modify the CLASS/MontePython numerical codes and consider the Planck18 CMB data (the TTTEEE likelihoods), the default BAO data as well as Lyα BAO data, the Pantheon SnIa compilation and a robust compilation of 18 RSD data.
- For the *LwMT* model we impose the priors $\Delta w \in [-0.7, 0.7]$ and $a_t \leq 0.99$ to obtain the following best fits

Parameter	best-fit	mean$\pm\sigma$	95.5% lower	95.5% upper
$\Omega_{m,0}$	0.3018	$0.3066^{+0.0064}_{-0.0065}$	0.2939	0.3196
H_0	68.56	$68.03^{+0.55}_{-0.58}$	66.94	69.15
σ_8	0.8141	0.8089 ± 0.0065	0.7957	0.8219
ΔM	-0.1676	-0.1698 ± 0.012	-0.1933	-0.1467
Δw	unconstrained	unconstrained	unconstrained	unconstrained
a_t	0.9856	> 0.985	> 0.984	> 0.984
$M_> \equiv M_c + \Delta M$	-19.408	-19.410 ± 0.012	-19.433	-19.387
$\chi^2_{\min}$	3834			

Result: The a_t (or equivalently z_t) reaches the highest (lowest) eligible value imposed by the prior and Δw seems to be neglected by the data.

G. Alestas, D. Camarena, E. Di Valentino, L. Kazantzidis, V. Marra, S. Nesseris and L. Perivolaropoulos, to appear in Phys.Rev.D.

Statistical Analysis Results (2/2)

For the LMT model, we set $\Delta w = 0$ and $z_t = 0.01$ and obtain the following best fits

For the LMT model, we set $\Delta w = 0$ and $z_t = 0.01$ and obtain the following best fits

Parameter	best-fit	mean$\pm\sigma$	95.5% lower	95.5% upper
$\Omega_{\mathrm{m},0}$	0.3088	$0.3082^{+0.0052}_{-0.0058}$	0.2976	0.3193
H_0	67.88	$67.89^{+0.42}_{-0.40}$	67.06	68.71
σ_8	0.8085	$0.8084^{+0.0058}_{-0.0061}$	0.7963	0.8205
ΔM	-0.170	-0.172 ± 0.012	-0.195	-0.149
$M_> \equiv M_c + \Delta M$	-19.410	-19.412 ± 0.012	-19.435	-19.389

$\chi^2_{\min}$	3835

Statistical Analysis Results (2/2)

For the *LMT* model, we set $\Delta w = 0$ and $z_t = 0.01$ and obtain the following best fits

Parameter	best-fit	mean$\pm\sigma$	95.5% lower	95.5% upper
$\Omega_{\mathrm{m},0}$	0.3088	$0.3082^{+0.0052}_{-0.0058}$	0.2976	0.3193
H_0	67.88	$67.89^{+0.42}_{-0.40}$	67.06	68.71
σ_8	0.8085	$0.8084^{+0.0058}_{-0.0061}$	0.7963	0.8205
ΔM	-0.170	-0.172 ± 0.012	-0.195	-0.149
$M_> \equiv M_c + \Delta M$	-19.410	-19.412 ± 0.012	-19.435	-19.389
χ^2_{min}	3835			

Result: We confirm that the introduction of Δw has basically no effect in the quality of fit. Moreover, the inferred value of $M_> = -19.41$ mag fully agrees with the CMB constraint of the absolute magnitude $M = -19.40$ mag.

G. Alestas, D. Camarena, E. Di Valentino, L. Kazantzidis, V. Marra, S. Nesseris and L. Perivolaropoulos, to appear in Phys.Rev.D.

Comparison of Different Dark Energy Models with a Flat Prior on M

- In order to truly resolve the Hubble crisis, a model should provide a consistent measurement with M_c at the 1σ level, but also a χ^2 value similar (or even better) to ΛCDM.

Comparison of Different Dark Energy Models with a Flat Prior on M

- In order to truly resolve the Hubble crisis, a model should provide a consistent measurement with M_c at the 1σ level, but also a χ^2 value similar (or even better) to ΛCDM.
- We consider the wCDM, the CPL, the PEDE as well as ΛCDM and impose a flat prior on the absolute magnitude $M \in [-19.28, -19.2]$ mag and find

Params	ΛCDM	wCDM	CPL	$LwMT$ ($z_t \geq 0.01$)	PEDE	LMT ($z_t = 0.01$)
$\Omega_{\rm m,0}$	$0.2564^{+0.0018}_{-0.0019}$	$0.2571^{+0.0019}_{-0.0020}$	$0.2719^{+0.0041}_{-0.0044}$	0.3066 ± 0.0063	0.2582 ± 0.0020	0.3082 ± 0.0053
H_0	72.40 ± 0.16	$73.99^{+0.26}_{-0.27}$	72.38 ± 0.48	68.03 ± 0.55	$73.90^{+0.17}_{-0.19}$	67.89 ± 0.40
σ_8	$0.8045^{+0.0072}_{-0.0081}$	$0.8507^{+0.0084}_{-0.0083}$	$0.8511^{+0.0084}_{-0.0081}$	0.8088 ± 0.0063	0.8517 ± 0.0059	0.8084 ± 0.0059
M	~ -19.28	~ -19.28	~ -19.28	$-19.24\,(M_<)$	~ -19.28	$-19.24\,(M_<)$
ΔM	-	-	-	-0.170 ± 0.011	-	-0.172 ± 0.011
$M_>$	-	-	-	-19.410 ± 0.011	-	-19.412 ± 0.011
Δw	-	-	-	unconstrained	-	-
a_t	-	-	-	> 0.987	-	-
w_0	-	$-1.162^{+0.021}_{-0.019}$	$-0.844^{+0.077}_{-0.089}$	-	-	-
w_a	-	-	$-1.27^{+0.38}_{-0.31}$	-	-	-
$\chi^2_{\rm min}$	3964	3889	3875	3834	3886	3835
$\Delta\chi^2_M$	-	-75	-89	-130	-78	-129

Comparison of Different Dark Energy Models with a Flat Prior on M

- In order to truly resolve the Hubble crisis, a model should provide a consistent measurement with M_c at the 1σ level, but also a χ^2 value similar (or even better) to ΛCDM.
- We consider the wCDM, the CPL, the PEDE as well as ΛCDM and impose a flat prior on the absolute magnitude $M \in [-19.28, -19.2]$ mag and find

Params	ΛCDM	wCDM	CPL	$LwMT$ $(z_t \geq 0.01)$	PEDE	LMT $(z_t = 0.01)$
$\Omega_{\mathrm{m},0}$	$0.2564^{+0.0018}_{-0.0019}$	$0.2571^{+0.0019}_{-0.0020}$	$0.2719^{+0.0041}_{-0.0044}$	0.3066 ± 0.0063	0.2582 ± 0.0020	0.3082 ± 0.0053
H_0	72.40 ± 0.16	$73.99^{+0.26}_{-0.27}$	72.38 ± 0.48	68.03 ± 0.55	$73.90^{+0.17}_{-0.19}$	67.89 ± 0.40
σ_8	$0.8045^{+0.0072}_{-0.0081}$	$0.8507^{+0.0084}_{-0.0083}$	$0.8511^{+0.0084}_{-0.0081}$	0.8088 ± 0.0063	0.8517 ± 0.0059	0.8084 ± 0.0059
M	~ -19.28	~ -19.28	~ -19.28	$-19.24\,(M_<)$	~ -19.28	$-19.24\,(M_<)$
ΔM	-	-	-	-0.170 ± 0.011	-	-0.172 ± 0.011
$M_>$	-	-	-	-19.410 ± 0.011	-	-19.412 ± 0.011
Δw	-	-	-	unconstrained	-	-
a_t	-	-	-	> 0.987	-	-
w_0	-	$-1.162^{+0.021}_{-0.019}$	$-0.844^{+0.077}_{-0.089}$	-	-	-
w_a	-	-	$-1.27^{+0.38}_{-0.31}$	-	-	-
$\chi^2_{\min}$	3964	3889	3875	3834	3886	3835
$\Delta\chi^2_M$	-	-75	-89	-130	-78	-129

Result: All models provide $M \sim -19.28$ mag, *i.e.* the lowest eligible value of the imposed prior and ΛCDM has the worse overall fit due to the fixed value of M.

Comparison of Different Dark Energy Models with a Gaussian Prior on M

- For the same dark energy models imposing a Gaussian prior on the absolute magnitude M of the form $M_c = -19.24 \pm 0.04$ mag we find

Parameters	ΛCDM	wCDM	CPL	$LwMT$ ($z_t \geq 0.01$)	PEDE	LMT ($z_t = 0.01$)
$\Omega_{\rm m,0}$	$0.3022^{+0.0051}_{-0.0052}$	0.2943 ± 0.0065	$0.2974^{+0.0067}_{-0.0068}$	$0.3073^{+0.0063}_{-0.0062}$	0.2789 ± 0.0049	0.3082 ± 0.0053
H_0	68.36 ± 0.4	69.47 ± 0.72	69.25 ± 0.73	67.96 ± 0.55	71.85 ± 0.45	67.89 ± 0.40
σ_8	$0.8076^{+0.0058}_{-0.0062}$	$0.8215^{+0.0095}_{-0.0097}$	$0.8248^{+0.0096}_{-0.0097}$	$0.8084^{+0.0064}_{-0.0065}$	0.8531 ± 0.0059	0.8085 ± 0.0057
S_8	$0.8105^{+0.0097}_{-0.01}$	0.8135 ± 0.0098	$0.8210^{+0.0107}_{-0.0106}$	0.8181 ± 0.0100	0.8226 ± 0.0095	0.8194 ± 0.0099
M	-19.40 ± 0.01	-19.38 ± 0.02	-19.37 ± 0.02	-19.26 ± 0.04	-19.33 ± 0.01	-19.24 ± 0.04
ΔM	-	-	-	$-0.145^{+0.038}_{-0.035}$	-	-0.168 ± 0.039
$M_>$	-	-	-	-19.410 ± 0.011	-	-19.411 ± 0.011
Δw	-	-	-	unconstrained	-	-
a_t	-	-	-	> 0.986	-	-
w_0	-	-1.050 ± 0.027	-0.917 ± 0.078	-	-	-
w_a	-	-	$-0.53^{+0.33}_{-0.28}$	-	-	-
$\chi^2_{\rm min}$	3854	3851	3848	3833	3867	3835
$\Delta\chi^2$	-	-3	-6	-21	$+13$	-19

Comparison of Different Dark Energy Models with a Gaussian Prior on M

- For the same dark energy models imposing a Gaussian prior on the absolute magnitude M of the form $M_c = -19.24 \pm 0.04$ mag we find

Parameters	ΛCDM	wCDM	CPL	$LwMT$ ($z_t \geq 0.01$)	PEDE	LMT ($z_t = 0.01$)
$\Omega_{\mathrm{m},0}$	$0.3022^{+0.0051}_{-0.0052}$	0.2943 ± 0.0065	$0.2974^{+0.0067}_{-0.0068}$	$0.3073^{+0.0063}_{-0.0062}$	0.2789 ± 0.0049	0.3082 ± 0.0053
H_0	68.36 ± 0.4	69.47 ± 0.72	69.25 ± 0.73	67.96 ± 0.55	71.85 ± 0.45	67.89 ± 0.40
σ_8	$0.8076^{+0.0058}_{-0.0062}$	$0.8215^{+0.0095}_{-0.0097}$	$0.8248^{+0.0096}_{-0.0097}$	$0.8084^{+0.0064}_{-0.0065}$	0.8531 ± 0.0059	0.8085 ± 0.0057
S_8	$0.8105^{+0.0097}_{-0.01}$	0.8135 ± 0.0098	$0.8210^{+0.0107}_{-0.0106}$	0.8181 ± 0.0100	0.8226 ± 0.0095	0.8194 ± 0.0099
M	-19.40 ± 0.01	-19.38 ± 0.02	-19.37 ± 0.02	-19.26 ± 0.04	-19.33 ± 0.01	-19.24 ± 0.04
ΔM	-	-	-	$-0.145^{+0.038}_{-0.035}$	-	-0.168 ± 0.039
$M_>$	-	-	-	-19.410 ± 0.011	-	-19.411 ± 0.011
Δw	-	-	-	unconstrained	-	-
a_t	-	-	-	> 0.986	-	-
w_0	-	-1.050 ± 0.027	-0.917 ± 0.078	-	-	-
w_a	-	-	$-0.53^{+0.33}_{-0.28}$	-	-	-
$\chi^2_{\min}$	3854	3851	3848	3833	3867	3835
$\Delta\chi^2$	-	-3	-6	-21	$+13$	-19

Result: The transition models perform better than the rest of the models, providing a consistent value with the Cepheid calibrated value M_c (the only ones) as well as a better quality of fit with respect to ΛCDM.

G. Alestas, D. Camarena, E. Di Valentino, L. Kazantzidis, V. Marra, S. Nesseris and L. Perivolaropoulos, to appear in Phys.Rev.D.

Summary and Conclusions

- Undoubtedly, we live in an exciting cosmological era. A plethora of alternative cosmological data in the last years hint towards the conclusion that the concordance model ΛCDM is not the end of the road and a new more complete theory of gravity is needed.

Summary and Conclusions

- Undoubtedly, we live in an exciting cosmological era. A plethora of alternative cosmological data in the last years hint towards the conclusion that the concordance model ΛCDM is not the end of the road and a new more complete theory of gravity is needed.
- All the models presented here have the potential to explain some of the basic problems of ΛCDM. We expect that the situation will be further clarified in the next decades, when new improved observational data from upcoming missions will be published.

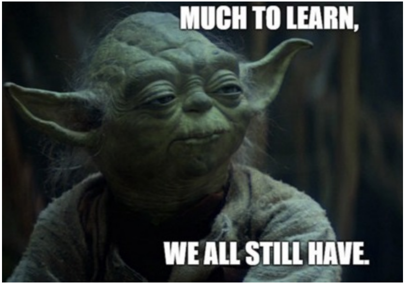

Thank you for your attention!

«This research is co-financed by Greece and the European Union (European Social Fund- ESF) through the Operational Programme «Human Resources Development, Education and Lifelong Learning» in the context of the project "Strengthening Human Resources Research Potential via Doctorate Research" (MIS-5000432), implemented by the State Scholarships Foundation (IKY)»

Ευρωπαϊκή Ένωση
European Social Fund

Operational Programme
Human Resources Development, Education and Lifelong Learning
Co-financed by Greece and the European Union

ΕΣΠΑ 2014-2020
ανάπτυξη - εργασία - αλληλεγγύη